

MODELING AND EXPERIMENTAL UPDATE ON QUASI-PHASE MATCHED DIRECT LASER ELECTRON ACCELERATION IN DENSITY-MODULATED PLASMA WAVEGUIDES *

M.-W. Lin, A. Rakhman, D. R. Abercrombie, and I. Jovanovic[†],

Department of Mechanical and Nuclear Engineering,
The Pennsylvania State University, University Park, PA 16802, U.S.A.

Abstract

Direct laser acceleration (DLA) of electrons using the axial electric field of a radially polarized, guided intense laser pulse has the potential to lead to compact laser-driven accelerators for security and medical applications. A density-modulated plasma waveguide could be applied to extend the laser beam propagation distance and to achieve quasi-phase matching (QPM) between laser and electron pulses for efficient DLA. We conducted numerical simulations to design the appropriate plasma structure of the waveguide and investigate the properties of accelerated electron beams. An all-optical method, based on the igniter-heater scheme for plasma waveguide fabrication, is experimentally implemented to machine the density-modulated plasma waveguides with low-Z gas targets. A novel angle-multiplexed diagnostic technique has been developed to extract the polarization state and temporal characteristics of a radially polarized femtosecond laser pulse using spatial-spectral interferometry. The goal of this work is to characterize the propagation of femtosecond radially polarized pulses in plasma waveguide, thus better predicting the DLA performance.

gas targets has been designed to experimentally produce density-modulated plasma waveguides. We studied the performance of the experimental system by generating laser-ionized nitrogen plasma columns in a gas jet, with data obtained from multiple diagnostics. An novel angle-multiplexed spatial-spectral interferometric technique has been demonstrated, capable of simultaneously reconstructing the phase and polarization of a femtosecond radially polarized laser pulses for use in DLA.

PIC SIMULATION OF DLA

In DLA realized in density-modulated plasma waveguides, the electron beam interacts with the electromagnetic field of the co-propagating laser pulse and the electrostatic field originating from the plasma. We carried out 3D simulations in order to understand the density profile and the energy spectrum of an accelerated electron beam. Each simulation is performed in a moving frame co-propagating with the laser pulse. The size of the simulation box is 23.38 μm in the axial direction (x) and 33.6 $\mu\text{m} \times 33.6 \mu\text{m}$

INTRODUCTION

Laser-based accelerators hold a significant promise to be considerably more compact and cheaper than their counterparts based on conventional technology. In direct laser acceleration (DLA), electrons are accelerated by the axial electric field of a guided, radially polarized laser pulse [1]. The peak field gradients on the order of tens of GV/m are expected from the drive laser pulses even below TW peak power. Density-modulated plasma waveguides [2] with axially periodic plasma density modulation could be used to extend the DLA accelerating distance and achieve quasi-phase matching (QPM) between the laser and electron pulses. We recently developed a test particle model of QPM DLA, in which a plasma waveguide has been modeled such that the laser pulse is guided with optimally designed axial structures to maximize the energy gain [3].

We report our progress on the development of a 3D particle-in-cell (PIC) simulation [4]. The simulation is performed for DLA of an injected 40 MeV mono-energetic electron beam in a density-modulated plasma waveguide. Based on the igniter-heater scheme for plasma waveguide fabrication [3], a laser machining setup for low-Z

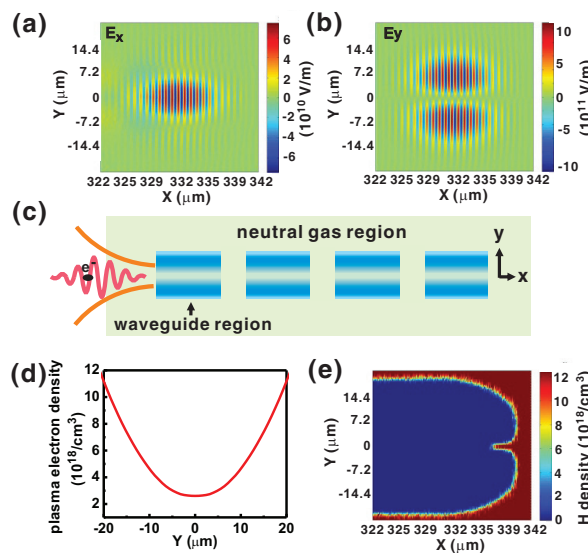


Figure 1: Snapshots of (a) longitudinal E_x and (b) transverse E_y electric fields of a 20-fs, 0.5-TW, radially polarized laser pulse in the PIC simulation; (c) illustration of a density-modulated plasma waveguide; (d) the transverse plasma density profile defined in the model for the waveguide regions; (e) ionization of neutral hydrogen gas by the electric field in (a) and (b).

* Work supported by the Defense Threat Reduction Agency.

[†] ijovanovic@psu.edu

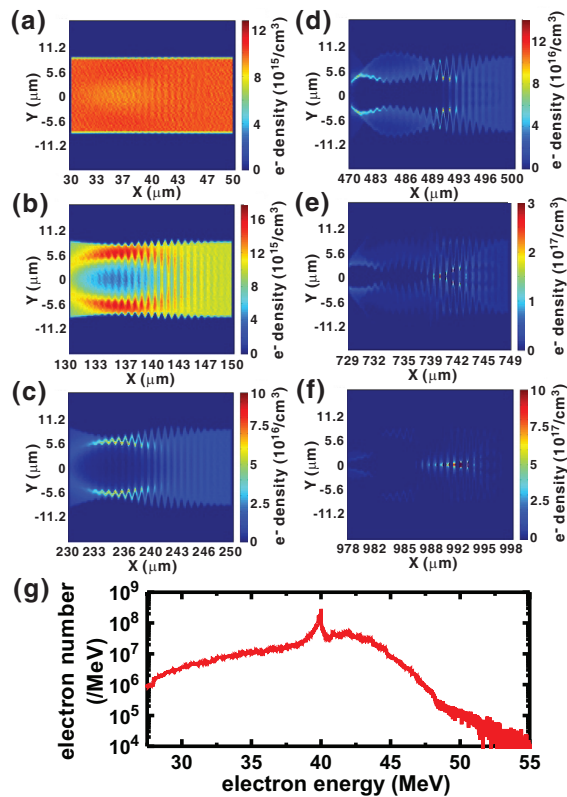


Figure 2: (a)-(f) Electron density and (g) the resulting energy spectrum of an electron beam injected with 40 MeV energy after propagating through a 1-mm long density-modulated plasma waveguide.

in the transverse direction (y and z). Figures 1(a) and (b) show the snapshots of the longitudinal E_x and transverse E_y components of the electric field of a 20-fs, 0.5-TW, radially polarized laser pulse in the simulation space. Alternating waveguide sections and neutral hydrogen gas sections are used to model a density-modulated plasma waveguide, as illustrated in Fig. 1(c). The waveguide sections have a transverse plasma density profile in which density increases quadratically in the transverse axis from the central density of $n_{e0}=2.5 \times 10^{18} \text{ cm}^{-3}$. The density profile shown in Fig. 1(d) defines a laser-guided mode radius of $w_0=8.5 \mu\text{m}$. Neutral hydrogen gas sections have a uniform density distribution with density $n_0=1.25 \times 10^{19} \text{ cm}^{-3}$. As shown in Fig. 1(e), hydrogen atoms can be fully ionized by the front foot of the 20-fs laser pulse.

We simulate the injection of a 40-MeV monoenergetic electron beam with cylindrical geometry having a radius $8.5 \mu\text{m}$ and length $19 \mu\text{m}$ into the plasma waveguide introduced previously. Considering the QPM condition, $300 \mu\text{m}$ and $100 \mu\text{m}$ are assigned respectively for the lengths of waveguide and neutral gas regions to match the corresponding dephasing lengths. The density of the electron beam is set to $1 \times 10^{16} \text{ cm}^{-3}$. Figures 2(a)-(f) show the variation of the density distribution when the electron beam

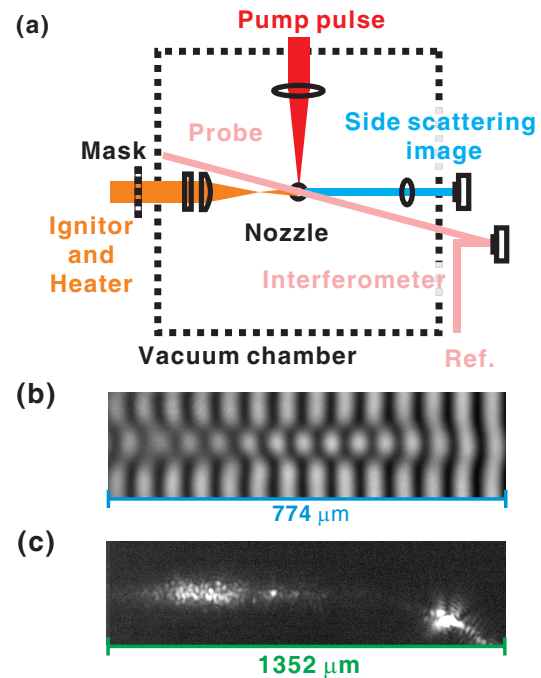


Figure 3: (a) Experimental layout of the plasma waveguide shaping system. (b) Interferogram and (c) side scattering image of a nitrogen plasma column produced by a laser pulse with the peak intensity $4.8 \times 10^{16} \text{ W/cm}^2$ and 700 psi backing pressure to the gas valve.

propagates through the 1-mm long plasma waveguide. It is observed that a density cavity forms at the back side of the electron beam due to the electrostatic force from the increased on-axis plasma electron density after the laser pulse. The ponderomotive force of the laser radial field pushes the background plasma electrons to concentrate in the center. As a result, the electron beam diverges where the plasma electrons pile up. This beam divergence prevents more electrons to remain in this region for effective DLA and finally reduces the fraction of electrons accelerated to higher energies. The final energy spectrum of the electron beam is shown in Fig. 2(g). Broadening of the energy spectrum depends on the injected electron phase.

THE PLASMA WAVEGUIDE SHAPING SYSTEM

Figure 3(a) shows the current DLA experimental layout. A gas with a low atomic number Z (e.g., hydrogen or helium) is used as the gas target. After passing through the mask, a 30-mJ, 40-fs ignitor pulse is horizontally imaged (with a demagnification factor of 10) and vertically focused by a cylindrical lens pair onto a neutral gas target. Using a spatially varying intensity pattern that is sufficiently intense to ionize the gas, plasmas with a relatively low electron density are produced where the laser intensity is sufficiently high. The waveguide is subsequently irradiated by another 200-ps, 200-mJ heater pulse, which heats and

fully ionizes the plasma through the inverse bremsstrahlung heating mechanism. The increased axial temperature allows the hydrodynamic expansion of plasma to take place from the center of this plasma column, lowering the on-axis electron density and forming a proper density profile to guide pump laser pulses in the longitudinal direction a few ns later. The mask pattern, the heater beam energy, and the time delay between the heater pulse and the radially polarized pump pulse need to be optimized for the QPM conditions for DLA.

We tested our experimental system by generating laser-ionized nitrogen plasma columns. The gas target was produced from a pulsed valve with a supersonic 1.4-mm long conical nozzle. Figure 3(b) is the interferogram of a nitrogen plasma column created by a 2.3-mJ, 40-fs linearly polarized laser pulse with 10- μ m focal spot diameter and 700-psi backing pressure to the gas valve. The corresponding side scattering image is shown in Fig. 3(c). The fringes in the recorded interferogram shift proportionally to the plasma density. It is estimated from the experimental data analyzed using the Abel inversion algorithm that the on-target peak electron density is approximately 10^{19} cm⁻³ at 100-psi backing pressure. The interferometer and the analysis of electron plasma density allows us to monitor the structure of the created plasma waveguide.

SPATIAL-SPECTRAL INTERFEROMETRY FOR PULSE CHARACTERIZATION

Spectral interferometry (SI) techniques, such as spatial encoded arrangement for temporal analysis by dispersing a pair of light E-fields (SEA TADPOLE) [5], can extract the spectral-phase difference between the signal pulse and the reference pulse. We extend this technique to an angularly multiplexed arrangement which enables simultaneous single-shot characterization of the temporal characteristics and the polarization of a radially polarized pulse. A spatial sample of the pulse is sent to an arrangement illustrated in Fig. 4(a), in which two orthogonally polarized reference beams are used. Horizontal and vertical components of the signal sample beamlets can interfere with each reference pulse independently at small angles (θ_1 and θ_2), producing interleaved fringes oriented along the spectral (horizontal) axis of the measurement. To extract the phase information, 1D Fourier transform of the interleaved interferogram along the spatial (vertical) axis yields four sidebands. These sidebands can be filtered in order to obtain the spectral-phase difference between the reference pulses and the signal pulse. The ratio of the amplitude of sidebands and the main peak (the DC term) provides the degree of polarization corresponding to the sampled beamlet.

For measurements, a \sim 20-fs, 800 nm laser pulse with a full-width at half-maximum bandwidth of \sim 70 nm was split into two reference pulses (with vertical and horizontal polarizations, respectively) and one signal pulse (polarized at 45° relative to the horizontal direction). The cross-

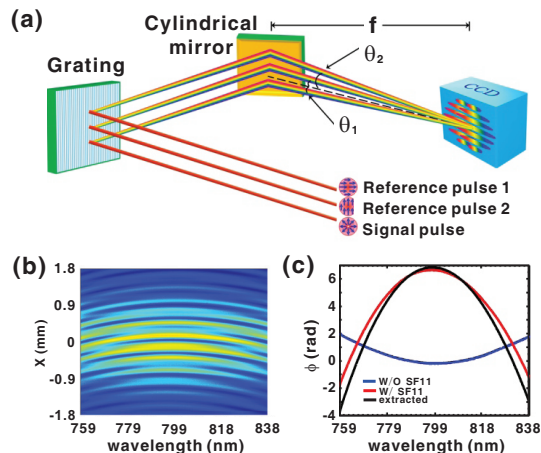


Figure 4: (a) Principle of the angle-multiplexed spatial-spectral interferometric technique. (b) The experimental interferogram with a 2-cm SF11 glass rod inserted in the beam and (c) the retrieved relative spectral phase.

ing angles between the signal and the two reference pulses are $\sim 0.1^\circ$ and $\sim 0.2^\circ$ into the CCD, respectively. Figure 4(b) shows the interferogram after a 2-cm SF11 glass was placed in the signal pulse path. The spectral phase difference between the signal beam and the reference beams was encoded in the interferogram. The retrieved spectral phase difference of the pulses is shown in Fig. 4(c). The measured GDD of 2063 fs²/cm is in reasonable agreement (8% error) with the dispersion calculated from the known Sellmeier coefficients as 1897 fs²/cm for 2-cm thick SF11 glass.

CONCLUSION

3D PIC simulations have been developed and are used to analyze QPM of DLA in density-modulated plasma waveguides. The simulations predict a divergent electron beam, reducing the fraction of electrons accelerated to high energies. Increasing the laser spot size [6] may be useful to reduce the space charge density and mitigate the beam divergence. A plasma shaping system has been designed and constructed and the plasma electron density in a gas target can be obtained from the diagnostic systems. A spatial-spectral interferometry technique has been developed for single-shot characterization of the phase and polarization state of a radially polarized pulse.

REFERENCES

- [1] P. Serafim, IEEE Trans. Plasma Sci. **28**, 1155 (2000).
- [2] A.G. York *et al.*, Phys. Rev. Lett. **100**, 195001 (2008).
- [3] M. -W. Lin and I. Jovanovic, Phys. Plasmas **19**, 113104 (2012).
- [4] C. Nieter and J. R. Cary, J. Comput. Phys. **196**, 448 (2004).
- [5] P. Bownan *et al.*, Opt. Express **14**, 11892 (2006).
- [6] S. J. Yoon, *et al.*, Phys. Rev. ST Accel. Beams **15**, 081305 (2012).